Nonlinear Dynamics **31:** 151–166, 2003.

Localized Basis Function Method for Computing Limit Cycle Oscillations

B. I. EPUREANU
Department of Mechanical Engineering, University of Michigan, Ann Arbor, MI 48109-2125, U.S.A.; E-mail: epureanu@umich.edu

E. H. DOWELL
Department of Mechanical Engineering and Materials Science, Duke University, Durham, NC 27708-0300, U.S.A.; E-mail: dowell@ee.duke.edu

(Received: 4 June 2002; accepted: 1 November 2002)

Abstract. An alternate approach to the standard harmonic balance method (based on Fourier transforms) is proposed. The proposed method begins with an idea similar to the harmonic balance method, i.e. to transform the initial set of differential equations of the dynamics to a set of discrete algebraic equations. However, as distinct from previous harmonic balance techniques, the proposed method uses a set of basis functions which are localized in time and are not necessarily sinusoidal. Also as distinct from previous harmonic balance methods, the algebraic equations obtained after the transformation of the differential equations of the dynamics are solved in the time domain rather than the frequency domain. Numerical examples are provided to demonstrate the performance of the method for autonomous and forced dynamics of a Van der Pol oscillator.

Keywords: Limit cycle computation, chaotic dynamics, time-domain, harmonic balance.

1. Introduction

Limit cycle oscillations are a common occurrence in many dynamical systems such as mechanical, electrical, and thermal systems. Predicting and characterizing such oscillations is of interest in a wide variety of design and analysis applications ranging from predicting chaotic dynamics [1] to analyzing rotor bearing systems [2, 3] and helicopter rotor dynamics [4] to aeroelasticity [5] and turbomachinery [6].

There are several techniques for computing limit cycle oscillations such as time integration, harmonic balance and shooting methods [7]. In particular, several variations of the harmonic balance method have been presented in the literature. Methods such as the classical and the incremental harmonic balance method [8] use direct Fourier transforms, while other methods, such as the fast Galerkin [9] and the alternating frequency-time domain techniques use fast Fourier transforms that have been shown to be more efficient computationally and easier to implement. Common to all these methods is that the original, time domain equations describing the dynamics are transformed to an alternate vector space, i.e. the Fourier space. The transformed set of equations is then truncated and a finite set of nonlinear algebraic equations is obtained. The unknowns in these equations are typically Fourier coefficients and they are solved by an iterative method such as Newton–Raphson, Broyden, and other methods. In this paper we present an alternate approach to the Fourier transform. The main idea of transforming the initial set of differential equations to a set of discrete algebraic equations is maintained. However, the set of basis functions used for the transformation are not necessarily sinusoidal

in time, but localized functions which are non-zero over a limited time interval. Moreover, the algebraic equations obtained after the transformation of the differential equations of the dynamics are solved in the time domain rather than the frequency domain.

The harmonic balance method has been applied to a wide variety of problems and is one of the techniques often used to study periodic solutions of nonlinear dynamical systems, i.e. limit cycles or forced responses especially because computing periodic solutions of nonlinear dynamical systems [10–14] is often critical for analysis, design, and control applications [15–17]. Thus, the harmonic balance method has been studied by researchers analyzing a broad range of fundamental problems such as predicting chaos [1], limit cycle oscillations [18–22], as well as other applications [2, 5, 23].

The early applications of the harmonic balance technique were based on harmonic balance equations obtained analytically, as part of the model [24, 25]. Later implementations used fast Fourier transforms of the nonlinear system of equations and proved to be more easily extended to a variety of problems since they did not require an analytic generation of the harmonic balance equations. Choi and Noah [26] used the Fourier transforms and an alternating frequency-time domain technique applied to piece-wise linear systems. However, their implementation requires analytical calculations when the nonlinearities present in the system are more complex. Cameron et al. [27] investigated an iterative method used in conjunction with the harmonic balance. The harmonic balance has also been used with an alternating frequency-time domain method, an extension of the fast Galerkin technique presented by Ling and Wu [9]. Aprile et al. [28] presented a generalized alternating frequency-time domain method where all nonlinearities from the equations describing the dynamics were lumped with the forcing terms. The resulting (virtual) forcing was then used to implement a standard fixed point iteration in the frequency domain while evaluating all nonlinearities in the time domain. Leung et al. [29] presented a faster algorithm for solving the equations obtained by Aprile et al. by implementing an alternating frequency-time domain method. The Toeplitz structure of the Jacobian was used in conjunction with a continuation algorithm in an otherwise classical alternating frequency-time domain implementation. Ren et al. [30] proposed a modified alternating frequency-time domain method for analyzing experimental data. Their method was designed for linear structures with localized nonlinear components. The Newmark time integration, the harmonic balance and the incremental harmonic balance [8] methods were discussed also.

In this paper, several key aspects of the standard multi-frequency harmonic balance method are presented first. Then, the alternate localized basis function method is proposed. The specific novel aspects of the proposed method are discussed and a comparison with the existing techniques is presented. Finally, numerical examples using the Van der Pol oscillator are provided to demonstrate the performance of the proposed method.

2. Standard Harmonic Balance

In general, a system of nonlinear ordinary differential equations describing the dynamics of a system may be expressed as

$$\mathbf{f}(\mathbf{x}, \dot{\mathbf{x}}, \ldots, t) = \mathbf{0}, \tag{1}$$

where $\mathbf{f}$ is an n-dimensional nonlinear function dependent on the vector of unknowns $\mathbf{x}$, its time derivatives $\dot{\mathbf{x}}$, $\ddot{\mathbf{x}}$, etc. and the time t. The period T of a periodic solution $\mathbf{x}_p$ is most often assumed known and the solution is written as a Fourier series

$$\mathbf{x}_p(t) = \sum_{i=-\infty}^{\infty} \mathbf{c}_i e^{i\omega t j}, \tag{2}$$

where $\omega = 2\pi/T$ is the fundamental frequency, $\mathbf{c}_i$ are complex Fourier vector coefficients, and $j = \sqrt{-1}$. The Fourier coefficients have complex conjugate values $\mathbf{c}_i = \mathbf{c}_{-i}^*$ when the state vector $\mathbf{x}$ is real.

The essence of the harmonic balance technique is to truncate the series in Equation (2) to a finite number of modes N and then substitute it into Equation (1). One then extracts the coefficients multiplying the terms $e^{i\omega t j}$ for all $i = 0 \ldots N$ from the newly obtained expression and sets them to zero obtaining

$$\mathbf{g}_i(T, \mathbf{c}_0, \ldots \mathbf{c}_N) = \mathbf{0}, \tag{3}$$

where the coefficients $\mathbf{c}_{-i}$ are replaced by $\mathbf{c}_i^*$ for all $i = 1 \ldots N$. Equation (3) represents a set of $N + 1$ nonlinear vector equations in the frequency domain that must be solved for the unknown coefficients $\mathbf{c}_i$, $i = 0 \ldots N$. The Newton–Raphson technique and the incremental harmonic balance are two of the methods often applied to solve Equation (3). When the period T of the limit cycle is unknown, one may use the same equations, by fixing the value of one of the coefficients $\mathbf{c}_k$ and solving for the period T along with the remaining N coefficients [9]. Some researchers have derived analytical expressions for Equation (3) for simple systems [24, 25]. However, Equation (3) is often obtained numerically rather than analytically due to the complexity of the Fourier transform of the nonlinearities.

Obtaining Equation (3) for given values of the Fourier coefficients $\mathbf{c}_k$ is one of the computationally expensive steps in implementing the harmonic balance technique. One approach to reduce the computational time required is to compute a time series of $\mathbf{f}$, perform a fast Fourier transform of this series [9, 26, 27], and extract a number of the Fourier coefficients of $\mathbf{f}$ which are precisely the values of $\mathbf{g}_i$. $N + 1$ of these coefficients are then used to complete the harmonic balance algorithm. When the solution of Equation (3) is obtained, the $N + 1$ values of $\mathbf{g}_i$ are very small and are considered the residual in the Newton–Raphson method [3]. In standard harmonic balance methods, Equation (3) is solved in the frequency domain. For complex functions $\mathbf{f}$ such as numerically known functions, the transformations of Equation (3) back to the time domain may be simplified by using fast Fourier transforms for example. Nevertheless, such transformations are computationally intensive and their frequent evaluation leads to longer computation time when compared to the finite element in time method [4, 6, 31, 32] or the localized basis function technique presented in this paper.

The nonlinear equations obtained in the frequency domain are solved most often by using general purpose nonlinear solvers. Several researchers [9, 27] investigated the Newton–Raphson approach and the Broyden method for the alternating frequency-time domain method. They noted that these methods fail under certain circumstances, and that more robust algorithms should be used. Indeed, even the most robust techniques available may fail to converge if the initial guess for a solution is not close enough to the desired solution [30]. In this paper we focus on the series truncation aspect of the method employed rather than on the specific nonlinear solver used. The localized basis function method is presented in the following section as an alternate approach to the frequency domain method or the classical time integration.

3. Localized Basis Function Method

One of the first steps performed in a harmonic balance method is to approximate the solution of the differential equation of the dynamics (Equation (1)) by a linear combination of complex exponential or sinusoidal functions. In this paper we propose an alternate method. Instead of using complex exponentials, we propose a different set of linearly independent basis functions. These basis functions are denoted by $b_i(\tau)$ and are functions of the non-dimensional time τ, where $\tau = t/T$, with T being the period of the limit cycle to be computed. The advantages and disadvantages of using various basis functions are discussed in the next section along with the reason for calling the proposed technique a localized basis function method.

Similar to the standard harmonic balance, the solution of Equation (1) may be approximated by

$$\mathbf{x}_p(t) = \sum_{i=0}^{N} \mathbf{c}_i b_i(t/T), \tag{4}$$

where $\mathbf{c}_i$ are unknown vector coefficients. When the period of the limit cycle to be computed is not known, the variable T is also unknown.

The series on the right hand side of Equation (4) is then truncated to a finite number of modes N and substituted into Equation (1). The time derivatives of the unknown vector $\mathbf{x}_p$ are computed based on the truncated series. For example, the first order derivative of $\mathbf{x}_p$ may be expressed as

$$\dot{\mathbf{x}}_p(t) = \frac{1}{T} \sum_{i=0}^{N} \mathbf{c}_i \dot{b}_i(t/T). \tag{5}$$

Substituting Equation (5) in Equation (1), one obtains an equation which has to hold for all time t. To form a set of N equations for the unknown coefficients $\mathbf{c}_i$, one then requires that Equation (5) be satisfied at N time instants θ_i. Thus, Equation (6) is obtained by requiring that Equation (1) be satisfied by the $\mathbf{x}_p$ given by Equation (5) at N distinct time instants θ_i. In the present analysis we chose θ_i to be exactly the time discretization instants t_i. However, these N time instants may be chosen differently without any major change in the implementation of the localized basis function method. Similar to Equation (3), one obtains

$$\mathbf{h}_i(T, \mathbf{c}_0, \ldots \mathbf{c}_N) = \mathbf{0}. \tag{6}$$

Distinct from the harmonic balance-type methods, in the localized basis function method the basis functions are not necessarily orthogonal although they are linearly independent. Thus, Equation (6) is not obtained by collecting the coefficients multiplying the basis functions and setting these coefficients to zero. But indeed Equation (6) is an equation for the coefficients $\mathbf{c}_i$ and the period T, *i.e.* coordinates of $\mathbf{x}_p$ in the transformed space. However, Equation (6) is expressed in the *time* domain, and not in the transformed domain. By operating in the time domain instead of the transformed space, the nonlinearities, the forcing terms and other aspects of the model formally expressed by Equation (1) are easier to handle. Additionally, transformations back and forth between the time domain and the transformed space are not necessary.

Also, Equation (4) does not depend explicitly on T because each basis function $\mathbf{b}_i(\tau)$ does not depend explicitly on T. Each basis function is specified for τ between zero and one,

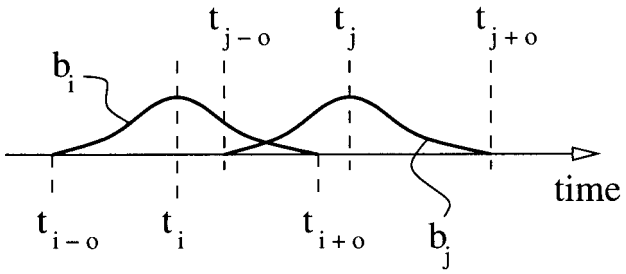

Figure 1. Basis functions b_i and b_j may overlap over at most o time intervals in the discretization.

where t/T lies. This implies that the shape of the basis function is independent of the period T. Nevertheless, Equation (6) does depend on T explicitly because the time derivatives of $\mathbf{x}_p$ depend explicitly on T as shown in Equation (5). The simple multiplicative dependence of Equation (6) upon $1/T$ is an added bonus leading to a simple form of the Jacobian in a Newton–Raphson implementation. In the next section we propose a set of basis functions and describe in more detail how these functions are used to obtain Equation (6).

4. Basis Functions

The basis functions used are non-zero over a small time interval, i.e. they are localized in time. One of the first steps in using such localized functions is to consider a number N_d of time discretization points which could be thought of as the zero reference for each basis function. The distribution of the time discretization points t_i is not restricted to be uniform during the period T. However, in the present analysis we have chosen a uniform distribution of t_i over the period T for simplicity. Re-scaling the time based on the period T of the limit cycle, and expanding the basis functions over the entire period, one obtains

$$b_i(\tau) = \begin{cases} 0, & \tau \le t_{i-o}/T, \\ q(\xi), & t_{i-o}/T < \tau < t_{i+o}/T, \\ 0, & \tau \ge t_{i+o}/T, \end{cases} \tag{7}$$

where ξ is a non-dimensional, re-scaled time variable given by $\xi = (\tau T - t_i)/(t_{i+o} - t_i)$ so that ξ varies between -1 and 1. The function $q(\xi)$ is chosen to be of the form $q(\xi) = k_1 + k_2\xi^2 + k_3\xi^4 + k_4\xi^6$ where the constants k_1, k_2, k_3 and k_4 were obtained based on smoothness and convergence arguments, which are discussed next. In addition, we used quadratic functions of ξ as basis functions and obtained a solution method similar to the finite element in time procedure. More details, numerical examples and results are presented in the next section. The index o indicates the number of time discretization points which two basis functions can overlap, as shown in Figure 1.

The choice of the precise shape of the function q is quite flexible. However, this function should have a few basic characteristics. Specifically, the magnitude of q is normalized by enforcing that $q(0) = 1$. Also, the function q is chosen to be zero for $\xi = -1$ and $\xi = 1$. In addition the function q was chosen to be an even function, i.e. $q(\xi) = -q(-\xi)$. The continuity of the derivative of the truncated series in Equation (5) was enforced, which implies that $\mathrm{d}q/\mathrm{d}\xi$ is zero for $\xi = -1$ and $\xi = 1$. Finally, the convergence of the method when N tends to infinity

was enforced. To obtain the requirement for q which will enforce convergence, an analysis based on finite differences has been done. Specifically, we used the following relation

$$\lim_{N\to\infty} \frac{\mathbf{x}_p(\theta_i + \Delta t) - \mathbf{x}_p(\theta_i - \Delta t)}{2\Delta t} = \frac{1}{T}\sum_{i=0}^{N} \mathbf{c}_i \dot{b}_i(\theta_i/T),$$

where $\Delta t = T/N$, while $\mathbf{x}_p(\theta_i + \Delta t)$ and $\mathbf{x}_p(\theta_i - \Delta t)$ are expressed using Equation (4). In addition, the coefficients c_i correspond to time instants t_i and thus $(c_{i+1} - c_{i-1})/2\Delta t$ tends to $\dot{c}_i$. Since q is an even function, after several algebraic manipulations, one obtains

$$\lim_{N\to\infty} \frac{1}{N}\sum_{i=0}^{N} q(i/N) - \frac{i}{N}\dot{q}(i/N) = 1. \tag{8}$$

One may alternatively express Equation (8) as

$$\int_{-1}^{1} q(\xi) - \xi q'(\xi)\,\mathrm{d}\xi = 1,$$

which implies that

$$\int_{-1}^{1} q(\xi)\,\mathrm{d}\xi = 1.$$

In the numerical examples presented in the next section, the constants k_1, k_2, k_3 and k_4 were determined using Equation (8).

An advantage of the localized basis function method is that the Jacobian $\partial\mathbf{h}/\partial\mathbf{c}_i$ necessary to solve Equation (6) is highly structured and sparse. The Jacobian is block $2 \times o$-diagonal, where o is the size of the largest overlap of any two basis functions. The size of each block is equal to the size of the vector $\mathbf{x}_p$, i.e. the number of coordinates. Thus, the Jacobian is easy to compute as it is sparse, requires few computations, and may be implemented in a simple numerical or analytical routine. For the example problem discussed in the following, the Jacobian is block o-diagonal, with o being tested for values ranging from 3 to 30. Also, the solution of the linear set of equations necessary to obtain during a Newton–Raphson (or other) Jacobian-based iterative solver may easily be computed because fast and simple routines for solving linear systems with block banded matrices are widely available.

Finally, consider the case where the function $\mathbf{f}$ does not depend explicitly on the time t, i.e. one has autonomous or free oscillations. In such a case, the period T is unknown and the $n \times N$ relations given by Equation (6) have to be solved for $n \times N + 1$ unknowns. However, the problem is easily solved by imposing a fixed, given value x_0 for the component r of $\mathbf{x}_p(t_m)$ at time index m, i.e. $\mathbf{x}_{p,r}(t_m) = x_0$. This technique is similar to the frequency domain technique proposed by Ling [9]. The index m corresponding to the fixed value of $\mathbf{x}_{p,r}(t_m)$ may have any value (in a given range) because the autonomous limit cycle is invariant to a translation in time. The index m simply establishes the phase of the oscillations. Thus, the starting time may be considered to have any value, and in particular a value such that $\mathbf{x}_{p,r}$ has the desired imposed value x_0 at time t_m. For example, one may set the value of the component $\mathbf{x}_{p,r}(0)$ to x_0 and consider that the time is measured starting from the index $i = 1$. Also, the necessary

known value x_0 is typically easy to estimate because the limit cycle is an oscillation of the system about a known static equilibrium value. A numerical example is given in the following section.

5. Numerical Examples

One of the nonlinear systems often investigated in the literature, the Van der Pol oscillator [19], is used to illustrate the proposed localized basis function technique. Due to its simplicity and rich dynamics, the Van der Pol oscillator provides a paradigm for many studies of limit cycle behavior and gives valuable insight regarding the localized basis function technique presented in the previous section. Both autonomous and forced Van der Pol oscillators are analyzed to demonstrate the generality and flexibility of the proposed approach. The equation of motion of a Van der Pol oscillator may be written as

$$\dot{z} + \mu(y^2 - 1)z + y - A\cos(2\pi t/T) = 0, \quad \dot{y} = z, \tag{9}$$

where y is a scalar function of the time t and represents the 'position' of the oscillator, μ is a constant which quantifies the level of nonlinearity, while A and T are the amplitude and the period of the forcing. For this system the dimension of the function $\mathbf{f}$ in Equation (1) is $n = 1$. Also, the autonomous Van der Pol oscillations may be studied by setting the forcing amplitude A to zero. In such a case the period of the limit cycle is unknown.

In all cases presented below the coefficient controlling the strength of the nonlinearity is $\mu = 2.375$. Other numerical calculations have been performed for various forcing amplitudes A, forcing periods T and levels of nonlinearity μ and in all cases the performance of the localized basis function method has been similar to the cases discussed below, but are not presented here for the sake of brevity. The Newton–Raphson iterative method has been used to solve the nonlinear equations obtained. Also, for the cases of autonomous oscillations, the Jacobian required in the Newton–Raphson method has been modified to account for the imposed fixed value x_0 at a fixed time index.

The discretization used $N = 200$ points while the constants k_1, k_2, k_3 and k_4 in the expression for q in Equation (7) were set to the following values:

$$o = 5 \rightarrow k_1 = 1, \quad k_2 = -3.17, \quad k_3 = 3.21, \quad k_4 = -1.11;$$

$$o = 10 \rightarrow k_1 = 1, \quad k_2 = -2.75, \quad k_3 = 2.51, \quad k_4 = -0.75;$$

$$o = 20 \rightarrow k_1 = 1, \quad k_2 = -2.59, \quad k_3 = 2.19, \quad k_4 = -0.59;$$

$$o = 30 \rightarrow k_1 = 1, \quad k_2 = -2.54, \quad k_3 = 2.09, \quad k_4 = -0.55.$$

Figures 2, 3, and 4 indicate in a very good agreement between the exact and the localized basis function solutions. The initial guesses for limit cycles used in the Newton–Raphson iterative process are shown by the dashed lines. The initial guess for the unknown period of the limit cycle was 6.5 while the exact value of the period is 8.071.

Calculations were performed for forced oscillations as well. The forcing period T of 5.026 corresponding to a forcing frequency ω of 1.25 has been considered. The forcing amplitude was $A = 2$ and the level of nonlinearity was $\mu = 2.375$. The forced Van der Pol oscillator has been found to have two co-existing limit cycles, a stable and an unstable limit cycle. The stable

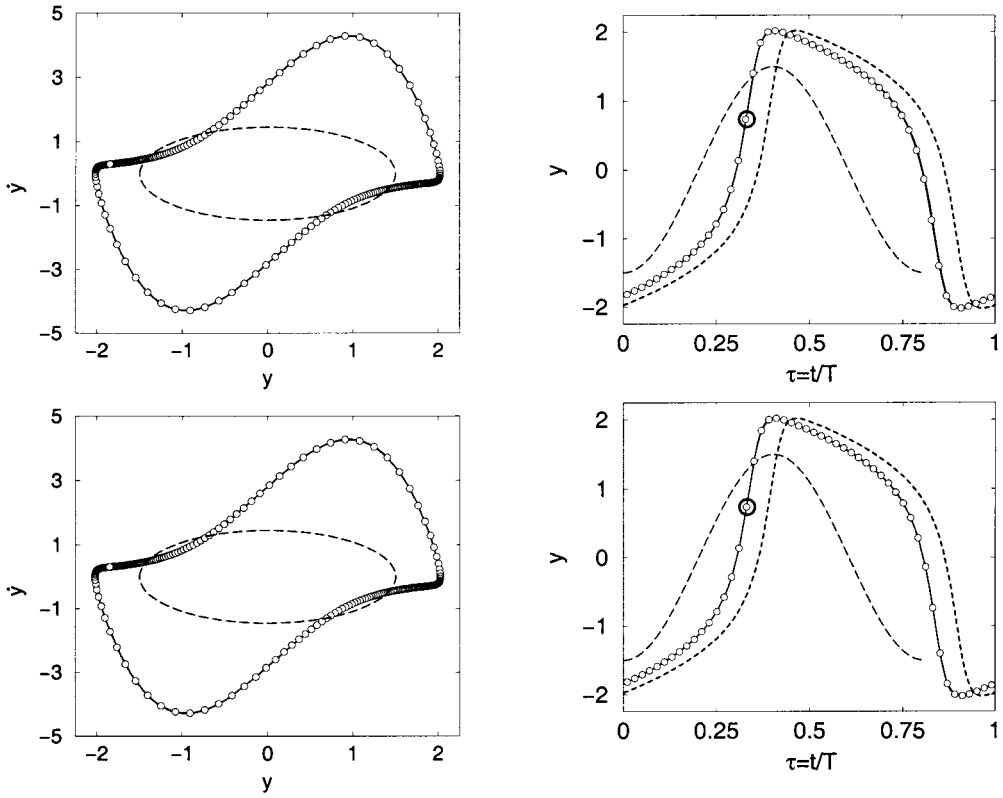

Figure 2. The dashed line represents the initial guess for the autonomous limit cycle. The symbols represent the limit cycle computed using the localized basis function method, while the solid line represents the exact limit cycle. The dotted line represents the exact limit cycle as computed using time integration without imposing the fixed location x_0 indicated by the thick circle. Results obtained for $o = 5$ and $o = 20$ are shown on the left, and $o = 10$ and $o = 30$ on the right.

limit cycle corresponds to a fixed point given by $y = -1.8737$, and $\dot{y} = 0.4503$ in a Poincaré map. The eigenvalues of the linearized Poincaré map around the fixed point have magnitudes 0.637 and 0.098, which are smaller than unity showing that the limit cycle is stable. In contrast, the unstable limit cycle corresponds to a fixed point given by $y = -0.1489$, and $\dot{y} = -0.9565$, while both eigenvalues of the linearized Poincaré map have magnitude 65.14. The stable and unstable exact limit cycles were computed using time integration and had a closure error of less than 10^{-9}.

To further test these results, we used quadratic interpolation functions $q(\xi)$ also. These functions lead to a solution method very similar to the finite element in time procedure. Specifically, a vector of unknowns $\mathbf{x}$ may be defined as a column vector composed of the positions $y(t_i)$ and velocities $\dot{y}(t_i) = z(t_i)$ at time instants t_i for $i = 1 \ldots N$. Thus, the vector $\mathbf{x}$ has dimension $2N$ and may be expressed as

$$\begin{aligned} \mathbf{x} &= [y(t_1) \ldots y(t_N)\ z(t_1) \ldots z(t_N)]^T \\ &= [y_1 \ldots y_N\ z_1 \ldots z_N]^T, \end{aligned} \tag{10}$$

where the superscript T indicates the transpose. The vector $\mathbf{x}$ is assumed to represent a quadratic interpolation of the limit cycle to be computed. The time instants are considered

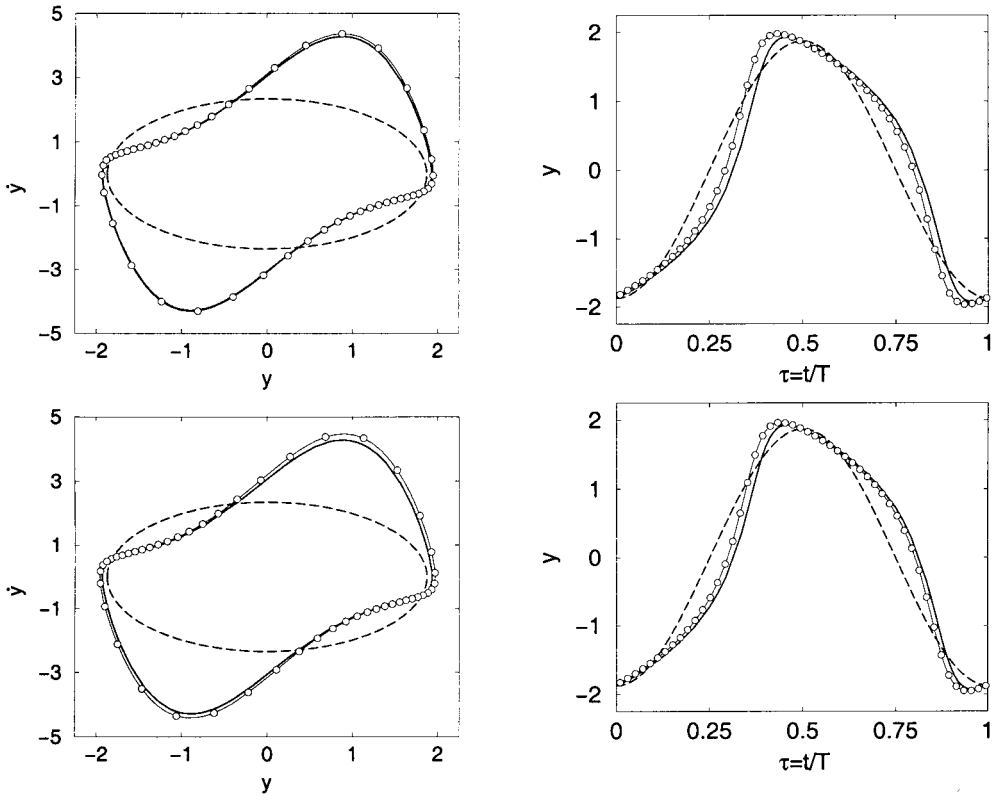

Figure 3. The dashed line represents the initial guess for the stable forced limit cycle. The symbols represent the forced limit cycle computed using the localized basis function method, while the solid line represents the exact limit cycle of the system. Results obtained for $o = 5$ and $o = 20$ are shown on the left, and $o = 10$ and $o = 30$ on the right.

uniformly distributed from time zero to T. The derivatives of y may then be approximated using finite difference as follows

$$\dot{x}_i = \frac{x_{i+1} - x_{i-1}}{2\Delta t}, \tag{11}$$

where x_i is the i-th component of the vector $\mathbf{x}$, and $\Delta t = T/N$. Substituting Equations (10) and (11) into Equation (9) for each time instant t_i, one obtains a set of N equations which are solved for $\mathbf{x}$.

When a non-uniform distribution of the time values t_i is used, then the finite differences in Equation (11) are not centered finite differences so that the derivatives at time t_i depend not only on the values of the unknowns $\mathbf{x}_p(t_{i+1})$ and $\mathbf{x}_p(t_{i-1})$, but also on $\mathbf{x}_p(t_i)$. However, these differences do not affect the general approach or the simplicity of the method.

The quadratic interpolation basis functions worked very well as shown in Figures 5, 6, 7 and 8. The autonomous solutions obtained using $N = 75$ and $N = 200$ are shown by the symbols in Figure 5. The exact limit cycles are indicated by the dotted and solid lines in Figure 5. The exact solutions were computed using an alternate technique based on time series of the dynamics, such that their closure error in a Poincaré map of the flow is less than 10^{-6}. The limit cycle computed using the time integration is indicated by the dotted lines. The fixed value x_0 has been set to $x_0 = -0.872$ for a time index $m = 45$ in the case where

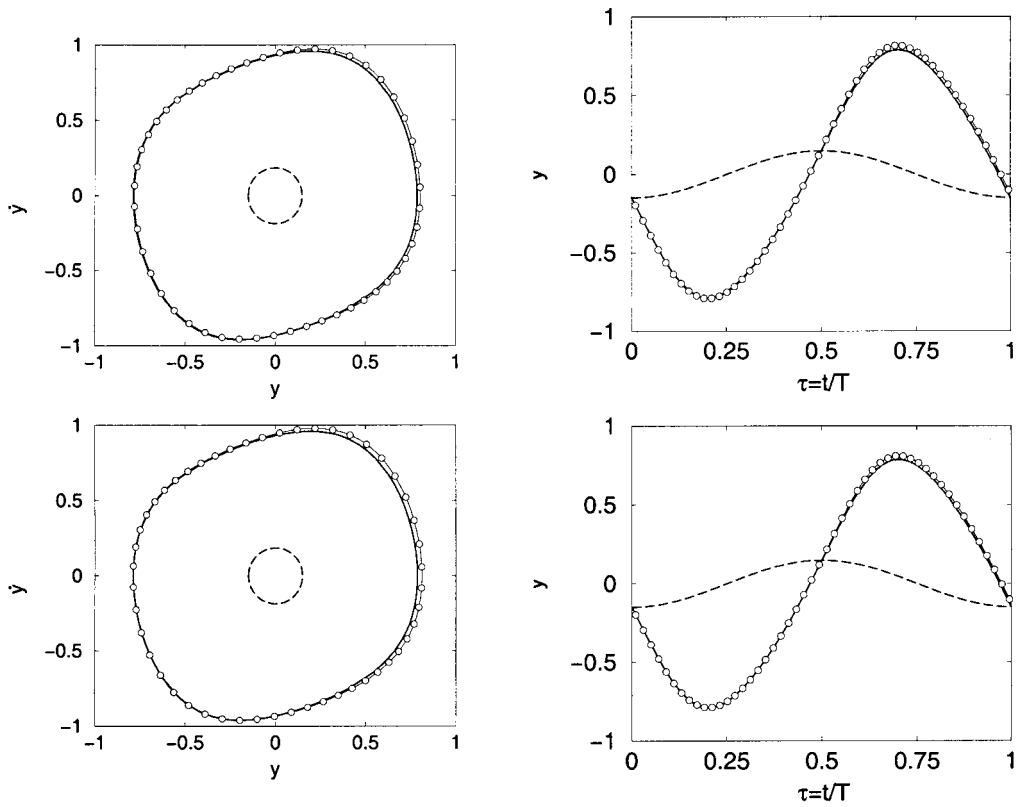

Figure 4. The dashed line represents the initial guess for the stable forced limit cycle. The symbols represent the forced limit cycle computed using the localized basis function method, while the solid line represents the exact limit cycle of the system. Results obtained for $o = 10$ and $o = 15$ are shown on the left, and $o = 20$ and $o = 30$ on the right.

$N = 75$ and $m = 120$ for the case where $N = 200$. The fixed value x_0 is indicated by the thick, large circles. Corresponding to each time index m, time integration has been used to obtain the exact solutions presented by the solid lines. A very good agreement between the exact and the localized basis function solutions was obtained. The initial guesses for limit cycles used in the Newton–Raphson iterative process are shown by the dashed lines. The initial guess for the unknown period of the limit cycle was 6.5. The exact value of the period is 8.071 and agrees very well with the values 7.952 and 8.057 obtained for $N = 75$ and $N = 200$ respectively, i.e. with an error of less than 1.5%. In both calculations, six iterations were required for convergence. The initial norm of the residual was of order unity or larger, and the final value was less than 10^{-11}.

Although the present method is derived starting from a harmonic balance point of view and then generalizing that approach to consider a broader class of (locally non-zero) basis functions in time rather than harmonic functions, it is interesting that the final results bear a similarity to the finite element in time approach. Note however that in the present method finite differences are used rather than finite elements and there is no appeal to a variational principle *per se*. That is, the original differential equations in time are solved directly using the localized basis function methodology.

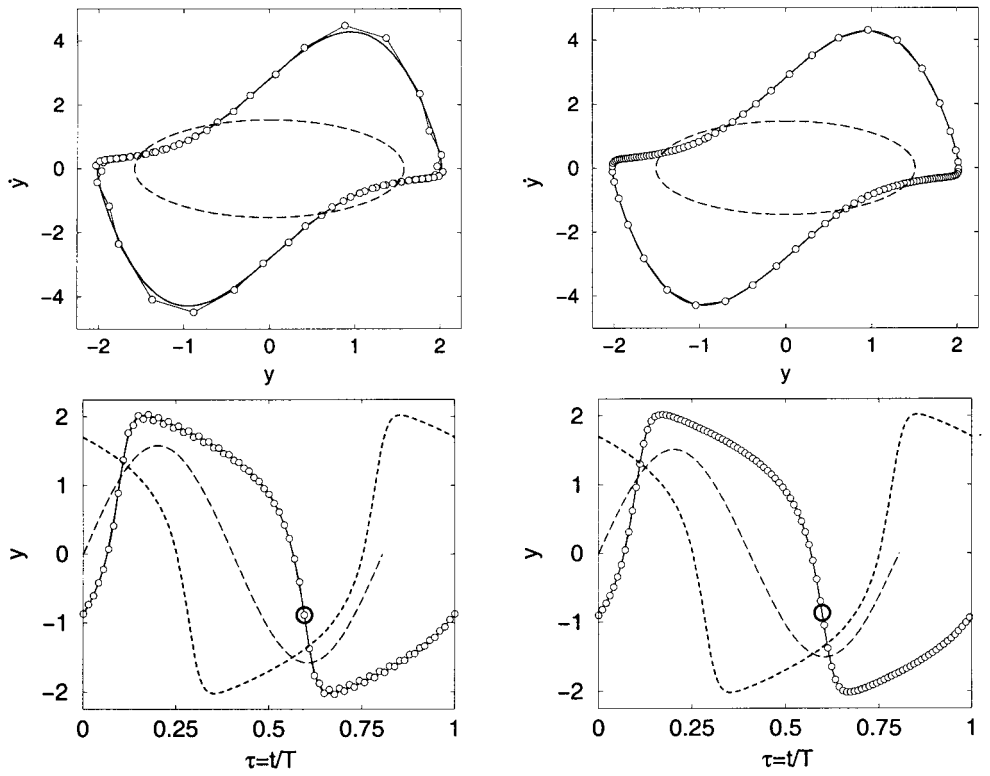

Figure 5. The dashed line represents the initial guess for the autonomous limit cycle. The symbols represent the limit cycle computed using the localized basis function method, while the solid line represents the exact limit cycle of the system. The dotted line represents the exact limit cycle as computed using time integration without imposing the fixed location x_0 indicated by the thick circle. Results obtained for $N = 75$ are shown on the left, and $N = 200$ on the right.

The forced limit cycle oscillations were computed using the localized basis function approach for $N = 45$, $N = 75$ and $N = 200$. In all cases, less than 10 Newton–Raphson iterations were required to reduce the initial norm of the residual from a value of order one or larger to values less than 10^{-12}.

The dashed lines in Figures 6 and 8 represent the state space plot of the initial guess for the forced limit cycles. The symbols represent the forced limit cycles computed using the localized basis function approach, while the solid lines represent the exact limit cycles of the system. Also, the dashed lines in Figures 6, 7 and 8 represent time series of the initial guesses for the forced limit cycles. The symbols represent the forced limit cycles computed using the localized basis function approach, while the solid lines represent the exact limit cycles of the system.

The effect of the time levels used in the localized basis function approach based on quadratic interpolation functions is indicated by the zig-zags observed at a small number $N = 45$ in Figure 8. The zig-zags obtained in the solution for $N = 45$ are drastically reduced when 75 time levels are used and completely removed when $N = 200$, as shown in Figures 6 and 7. These zig-zags did not appear for the other type of basis function, i.e. $q(\xi) = k_1 + k_2\xi^2 + k_3\xi^4 + k_4\xi^6$.

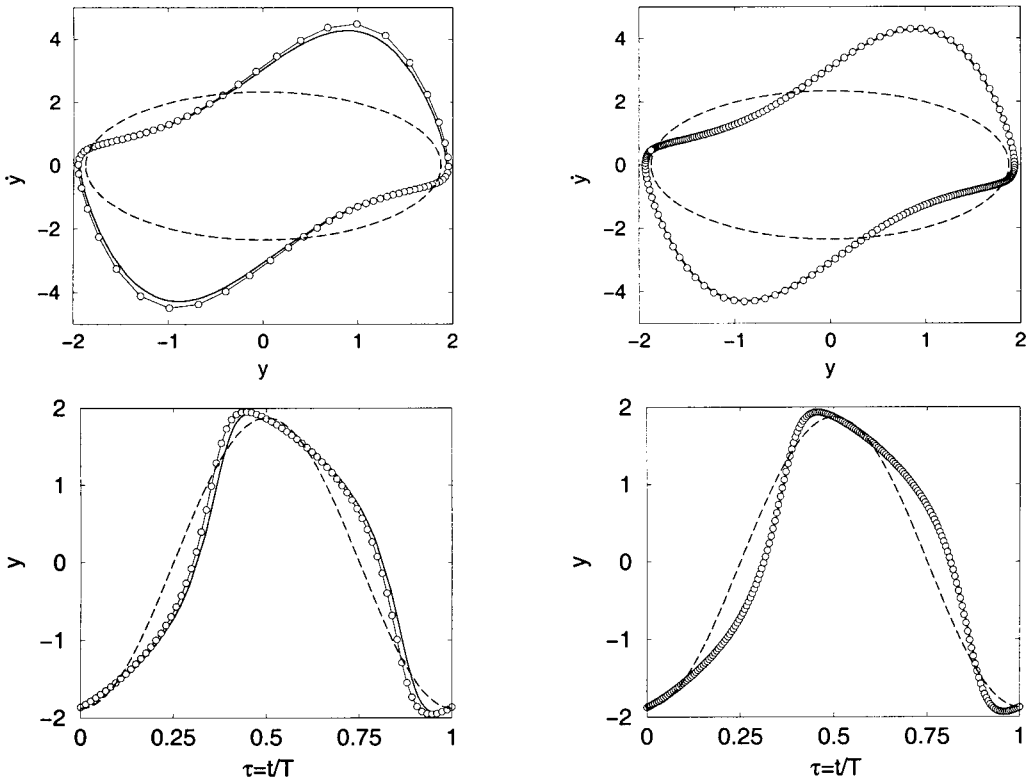

Figure 6. The dashed line represents the initial guess for the stable forced limit cycle. The symbols represent the forced limit cycle computed using the localized basis function method, while the solid line represents the exact limit cycle of the system. Results obtained for $N = 75$ are shown on the left, and $N = 200$ on the right.

An advantage of the proposed method over the standard harmonic balance method is that it does not require an iterative alternation between the time and frequency domains. This alternation may be done efficiently by using fast Fourier transforms [26]. However, the computational time necessary is still quite large, especially when large problems are tackled. Furthermore, the proposed method has been found to be better suited for use with Newton–Raphson iterations for the Van der Pol oscillator example (both forced and autonomous cases). The standard harmonic balance based on fast Fourier transforms has been applied to the numerical example presented and various numerical difficulties have been encountered in the iterative process. In contrast, the proposed method has converge easily in approximately 10 iterations.

In all cases presented, the final residual was very small although the initial residual was large. This suggests that the convergence properties of the Newton–Raphson method are acceptable for this problem. In the following we discuss the main results demonstrated and present the principal characteristics of the localized basis function method as distinct from fast Galerkin, alternating time-frequency and standard harmonic balance methods.

6. Discussion and Conclusions

There are several advantages of the localized basis function method as compared to the fast Galerkin and the alternating frequency-time domain techniques. One of the most significant

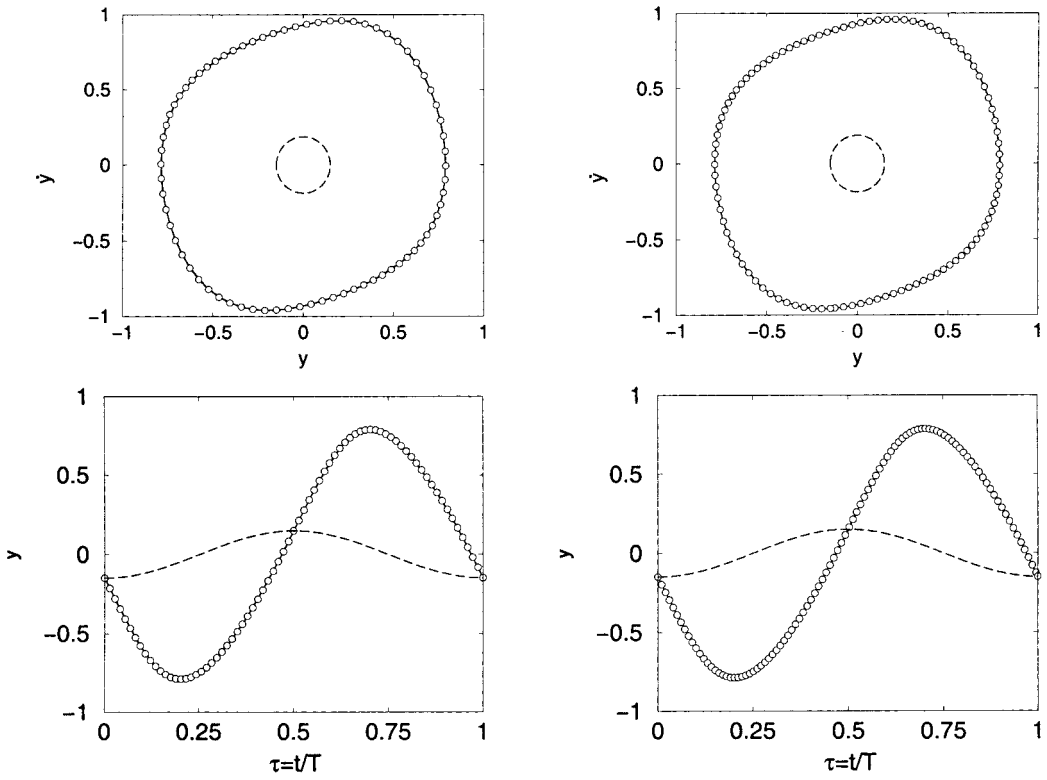

Figure 7. The dashed line represents the initial guess for the unstable forced limit cycle. The symbols represent the forced limit cycle computed using the localized basis function approach, while the solid line represents the exact limit cycle of the system. Results obtained for $N = 75$ are shown on the left, and $N = 200$ on the right.

is that the computation time required by the localized basis function approach grows linearly with N instead of $N^2 \log N$ or N^2 as in the other methods. The growth is linear because only systems of linear equations with o-diagonal matrices have to be solved at each iteration. The method works for autonomous as well as non-autonomous, forced systems and is equally applicable to problems where sub-harmonics or super-harmonics are to be calculated.

The localized basis function method to some extent resembles the alternating time-frequency method, but it is significantly different. An important difference is that the basis functions used are fundamentally different, i.e. localized functions are used instead of sinusoidal functions. Additionally, the computation of the limit cycle is different and the iterative solution method is different because the localized basis function method operates in the time domain only, rather than both time and frequency domains.

The various implementations of the localized basis function method are essentially embedded in the definition of the basis functions and the time instants θ_i. Thus, the localized basis function method is easily implemented in a modular fashion so that it may be tailored to the specifics of each application. Also, the method proposed works for basis functions where the time sampling is not uniform, unlike most fast Fourier transform based approaches. The non-uniformity of the time samples is advantageous because in some applications the dynamics may need to be resolved finely only during certain parts of the limit cycle, and not uniformly throughout the period.

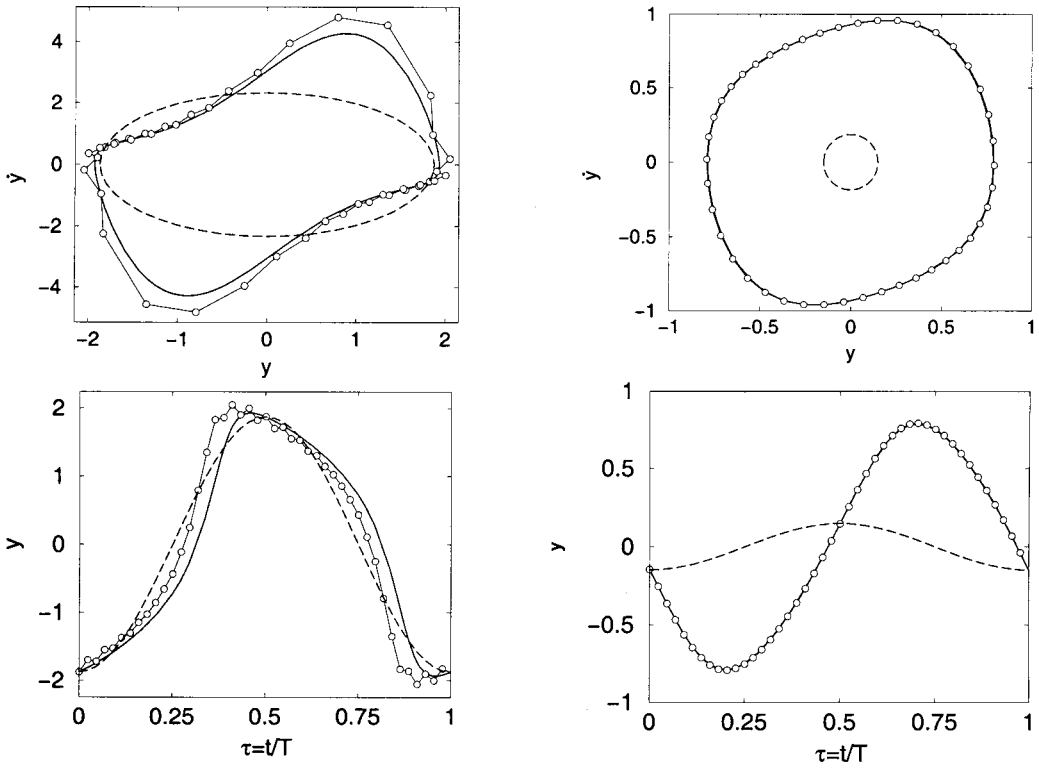

Figure 8. The dashed line represents the initial guess for the forced limit cycle. The symbols represent the forced limit cycle computed using the localized basis function approach with $N = 45$, while the solid line represents the exact limit cycle of the system. Results obtained for the stable limit cycle are shown on the left, and for the unstable limit cycle on the right.

The proposed approach is well suited for solving problems where coupled systems of equations are involved. The presence of coupled equations increases the size of each block in the Jacobian $\partial \mathbf{h}/\partial \mathbf{c}_i$ because the coupled equations increase the size of the vector $\mathbf{x}_p$. However, the block structure of the Jacobian is maintained and the advantages of such a structure can still be exploited. More complex problems involving partial differential equations have been investigated and very good results have been obtained. Several preliminary results have been obtained for a chaotic aeroelastic system [33] which lead to a set of 50 to 100 strongly coupled equations investigated using a set of basis functions with only one overlap ($o = 1$) and other techniques beyond the scope of this paper. These results are omitted here for the sake of brevity.

A Newton–Raphson iterative method has been applied to the numerical equations obtained and a fast and easy to implement algorithm has been presented, providing a useful and general tool for studying complex nonlinear dynamic systems. The contribution of the method proposed is not the use of the Newton–Raphson method *per se*, but rather the idea of using alternative basis functions when approximating the shape of the limit cycle. Also, the method proposed may be used in conjunction with the method presented by Leung [29] when the localized basis functions lead to a Toeplitz structure of the Jacobian. To implement the localized basis function method, any iterative or direct method may be used although the direct solvers may require large memory storage during computations. In the numerical examples presen-

ted, we used Newton–Raphson iterations. Methods such as pseudo-time marching, Broyden method, or other iterative methods may be used as well.

The localized basis function method is based on an appropriate selection of the basis functions for the dynamical system analyzed. The classical approach postulates a shape for such functions, i.e. sinusoidal shapes. For some problems, the sinusoidal shapes are a good, rational choice. However, for several problems, sinusoidal shapes are not a very good choice. The localized basis function approach is a flexible, more general method which allows the implementation of various basis functions which may be a better choice for each specific application.

For the case where the basis functions are quadratic interpolation functions, the method proposed bears a similarity to the finite element in time approach. However, in the localized basis function methodology, there is no appeal to a variational principle *per se* and the limit cycles are computed using the original differential equations in the time domain directly.

References

1. Gilli, M. and Maggio, M., 'Predicting chaos through an harmonic balance technique: An application to the time-delayed Chua's circuit', *IEEE Transactions on Circuits and Systems* **43**, 1996, 872–874.
2. Hahn, E. J. and Chen, P. Y. P., 'Harmonic balance analysis of general squeeze film damped multidegree-of-freedom rotor bearing systems', *Journal of Tribology* **116**, 1994, 499–507.
3. Nataraj, C. and Nelson, H. D., 'Periodic solutions in rotor dynamic systems with nonlinear supports: A general approach', *Journal of Sound and Vibration* **111**, 1989, 187–193.
4. Borri, M., 'Helicopter rotor dynamics by finite element in time approximation', *Computers and Mathematics with Apprications* **12A**, 1986, 149–160.
5. Matsuzaki, Y., 'Reexamination of stability of a two-dimensional finite panel exposed to an incompressible flow', *Journal of Applied Mechanics* **48**, 1981, 472–478.
6. Wang, Y., 'Stick-slip motion of frictionally damped turbine airfoils: A finite element in time (FET) approach', *Journal of Vibration and Acoustics* **119**, 1997, 236–242.
7. Holodniok, M. and Kubicek, M., 'DERPER – An algorithm for the continuation of periodic solutions in ordinary differential equations', *Journal of Computational Physics* **55**, 1984, 254–267.
8. Pierre, C., Ferri, A. A., and Dowell, E. H., 'Multi-harmonic analysis of dry friction damped systems using an incremental harmonic balance method', *Journal of Applied Mechanics* **52**, 1985, 958–964.
9. Ling, F. H. and Wu, X. X., 'Fast Galerkin method and its application to determine periodic solutions of non-linear oscillators', *International Journal of Non-Linear Mechanics* **22**, 1987, 89–98.
10. Guckenheimer, J. and Holmes, P., *Nonlinear Oscillations, Dynamical Systems, and Bifurcations of Vector Fields*, Springer-Verlag, New York, 1983.
11. Moon, F. C., *Chaotic and Fractal Dynamics: An Introduction for Applied Scientists and Engineers*, Wiley, New York, 1992.
12. Ott, E., *Chaos in Dynamical Systems*, Cambridge University Press, New York, 1993.
13. Strogatz, S. H., *Nonlinear Dynamics & Chaos*, Addison-Wesley, Reading, MA, 1994.
14. Wiggins, S., *Introduction to Applied Nonlinear Dynamical Systems and Chaos*, Springer-Verlag, New York, 1990.
15. Epureanu, B. I. and Dowell, E. H., 'System identification for Ott–Grebogi–Yorke controller design', *Physical Review E* **56**, 1997, 5327–5331.
16. Epureanu, B. I. and Dowell, E. H, 'On the optimality of the OGY control scheme', *Physica D* **116**, 1998, 1–7.
17. Epureanu, B. I., Trickey, S. T., and Dowell, E. H., 'Stabilization of unstable limit cycles in systems with limited controllability: Expanding the basin of convergence of OGY-type controllers', *Nonlinear Dynamics* **15**, 1998, 191–205.
18. Basso, M., Genesio, R., and Tesi, A., 'A frequency method for predicting limit cycle bifurcations', *Nonlinear Dynamics* **13**, 1997, 339–360.
19. Cunningham, W. J., *Introduction to Nonlinear Analysis*, McGraw-Hill, New York, 1958.

20. Garcia-Margallo, J. and Bejarano, J. D., 'The limit cycles of the generalized Rayleigh–Lienard oscillator', *Journal of Sound and Vibration* **156**, 1992, 283–301.
21. Piccardi, C., 'Bifurcations of limit cycles in periodically forced nonlinear systems: the harmonic balance approach', *IEEE Transactions on Circuits and Systems* **41**, 1994, 315–320.
22. Piccardi, C., 'Harmonic balance analysis of codimension-two bifurcations in periodic systems', *IEEE Transactions on Circuits and Systems* **43**, 1996, 1015–1018.
23. Yuen, S. W. and Lau, S. L., 'Effects of in-plane load on nonlinear panel flutter by incremental harmonic balance method', *AIAA Journal* **29**, 1991, 1472–1479.
24. Lau, S. L., Cheung, Y. K., and Wu, S. Y., 'Incremental harmonic balance method with multiple time scales for aperiodic vibration of nonlinear systems', *Journal of Applied Mechanics* **50**, 1983, 871–876.
25. Moiola, J. and Chen, G., 'Computation of limit cycles via higher order harmonic balance approximation', *IEEE Transactions on Automatic Control* **38**, 1993, 782–790.
26. Choi, Y. S. and Noah, S. T., 'Forced periodic vibration of unsymmetric piecewise-linear systems', *Journal of Sound and Vibration* **121**, 1988, 117–126.
27. Cameron, T. M. and Griffin, J. H., 'An alternating frequency/time domain method for calculating the steady-state response of nonlinear dynamic systems', *Journal of Applied Mechanics* **56**, 1989, 149–154.
28. Aprile, A., Benedetti, A., and Trombetti, T., 'On non-linear dynamic analysis in the frequency domain: Algorithms and applications', *Earthquake Engineering and Structural Dynamics* **23**, 1994, 363–388.
29. Leung, A. Y. T. and Ge, T., 'Toeplitz Jacobian matrix for nonlinear periodic vibration', *Journal of Applied Mechanics* **62**, 1995, 709–717.
30. Ren, Y. and Beards, C. F., 'A new receptance-based perturbative multi-harmonic balance method for the calculation of the steady state response of non-linear systems', *Journal of Sound and Vibration* **172**, 1994, 593–604.
31. Peters, D. A. and Izadpanah, A. P., 'hp-version finite elements for space-time domain', *Computational Mechanics* **3**, 1988, 73–78.
32. Warner, M. S. and Hodges, D. H., 'Solving boundary-value problems using hp-version finite elements in time', *International Journal for Numerical Methods in Engineering* **43**, 1998, 425–440.
33. Epureanu, B. I. and Dowell, E. H., 'Compact methodology for computing limit cycle oscillations in aeroelasticity', *Journal of Aircraft*, 2002, to appear.